ACS APPLIED MATERIALS & INTERFACES

Letter

www.acsami.org

Novel Composite Layer Based on Electrospun Polymer Nanofibers for Efficient Light Scattering

Hyun Jun Lee,[†] Seongpil An,[‡] Ju Hyun Hwang,[†] Sun-Gyu Jung,[†] Hong Seok Jo,[‡] Kyu Nyun Kim,[†] Yong Sub Shim,[†] Cheol Hwee Park,[†] Sam S. Yoon,[‡] Young Wook Park,*[,§] and Byeong-Kwon Ju*[,†]

[†]Display and Nanosystem Laboratory, College of Engineering, [‡]School of Mechanical Engineering, College of Engineering, and [§]The Institute of High Technology Materials and Devices, Korea University, Seoul 136-713, Republic of Korea

Supporting Information

ABSTRACT: We fabricated a PAN (polyacrylonitrile) NF (nanofiber)-embedded composite layer to adjust the light-control layer in light-emitting-diode (LED) and organic-light-emitting-diode (OLED) lighting systems with unique optical characteristics, for effective light scattering. The newly designed light-control composite layers with a composition of PAN NF/SU-8 exhibited a change in the optical properties, which was identified by the diameter control of the NF using a simple process. The change in the optical properties was largely dependent on the embedded NF's features. Therefore, the NF can be applied in different types of lighting systems, depending on each lighting device's purpose.

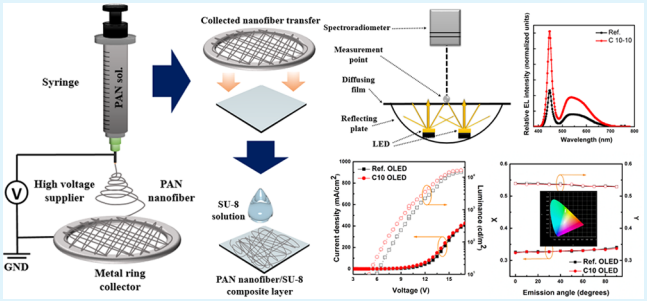

KEYWORDS: *electrospun nanofibers, composite layer, light scattering, light-emitting diodes (LEDs), organic light-emitting diodes (OLEDs)*

Rapid advances in micro and nano technology have contributed to the growth of the high-tech industry and created a new market in a short period of time.[1] The display industry is expected to see a high market share with the innovative evolution of the light-emitting diode (LED), including high-quality organic light-emitting diodes (OLEDs).[2,3] This remarkable growth will lead to an increase in the competition as well as market saturation, and it may be time to broaden our perspectives regarding LEDs and OLEDs. To achieve further success in the lucrative lighting market, LEDs and OLEDs must satisfy the rapidly changing market demands. Henceforth, the lighting system is expected to play a leading role in the LED market, provide higher efficiency applications, replace incandescent light bulbs, and lead to technological progress. Also, OLED lighting systems will enter the market as soon as the opportunity arises. However, both of these lighting systems face challenges for their ideal application. Therefore, new lighting system candidates with low-cost production must be developed to suit various customer requirements. For example, LEDs may feature a precisely designed light diffusion plate in order to avoid the glare effect, for the effective distribution of the light source. According to one report, LED light with a strong glare may

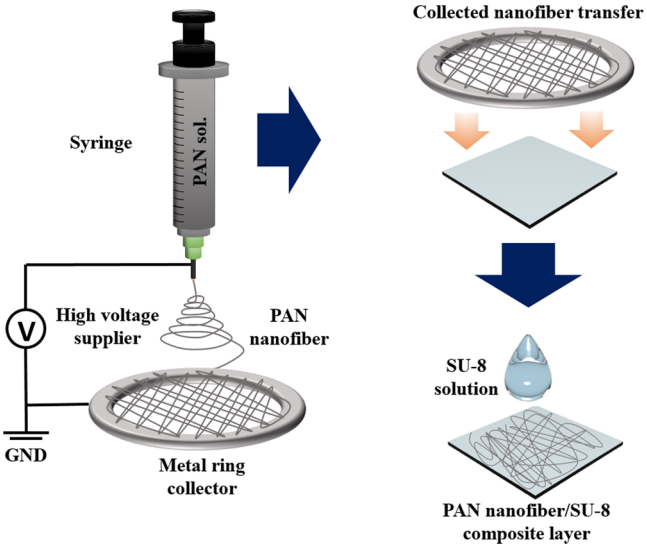

Figure 1. Schematic of the composite film for the PAN/SU-8 composite film with electrospinning fabrication process.

Table 1. PAN NF Production Conditions with Respect to PAN Concentration

sample	flow rate (μL/h)	applied voltage (kV)	diameter size (nm)
PAN 6 wt % NF	50	4.5	150
PAN 8 wt % NF	150	5	300
PAN 10 wt % NF	200	5	600

Received: October 30, 2014
Accepted: December 12, 2014
Published: December 12, 2014

ACS Publications © 2014 American Chemical Society

DOI: 10.1021/am5075387
ACS Appl. Mater. Interfaces 2015, 7, 68−74

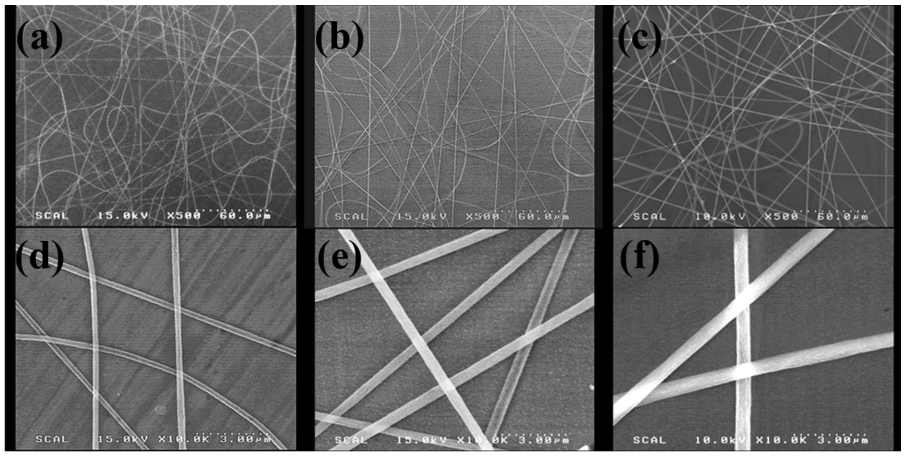

Figure 2. SEM images of PAN NF fabricated with different PAN weight ratios of (a, d) 6, (b, e) 8, and (c, f) 10 wt %.

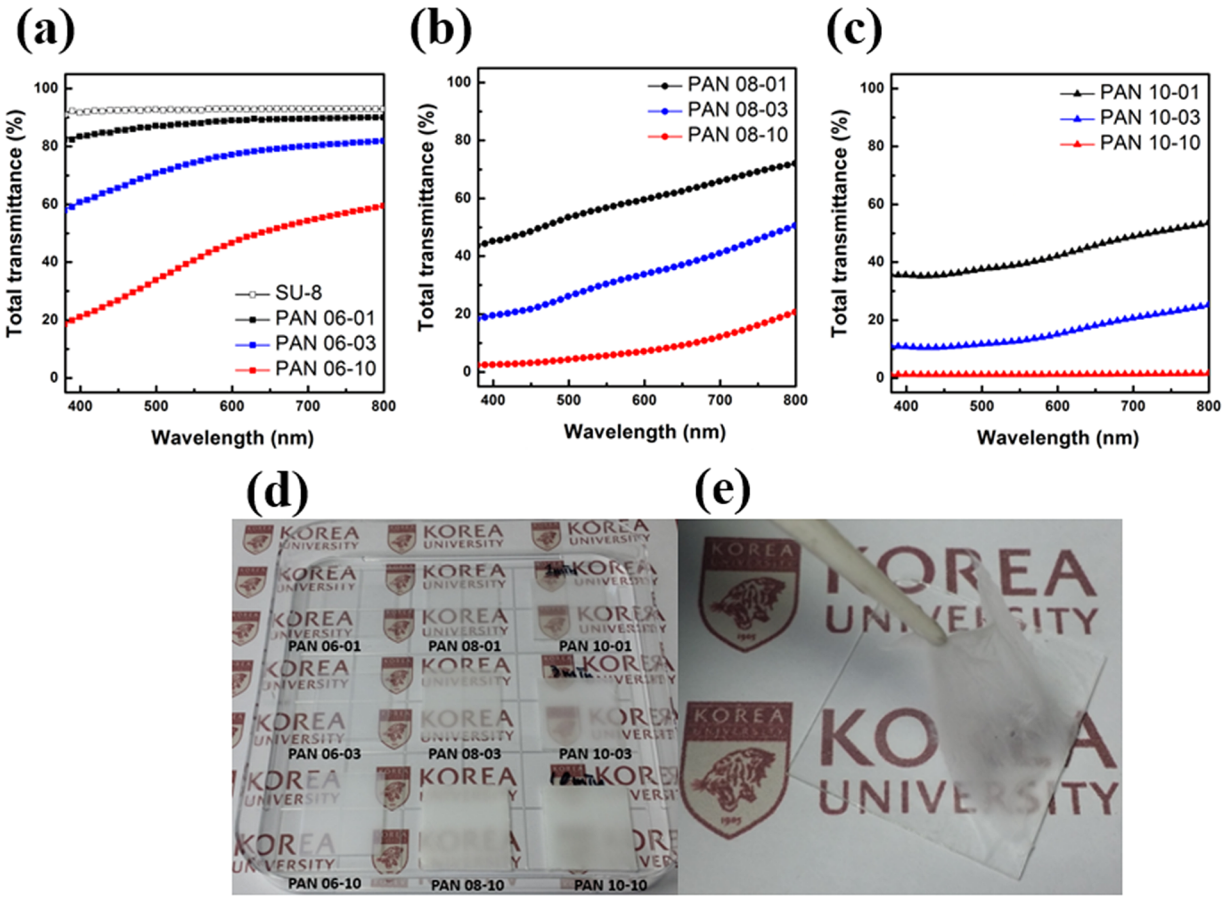

Figure 3. Optical characteristics of pristine PAN NF films: (a–c) Total optical transmittance of the SU-8 and various PAN NF films; (d) image of the PAN NF films; and (e) peel-off-test image of the PAN NF layer.

damage the retinal pigmented epithelial.[4] Therefore, the strong light of LEDs requires an effective diffusion layer providing the appropriate light distribution for the antiglare effect. Another example is the light-outcoupling enhancement technology for OLEDs. The light extraction of OLEDs incorporating unique structure compositions and newly designed additional layers has been examined using techniques such as the micro lens array,[5] random pattern,[6] and optically optimized device model.[7] Because of the efficiency and stability required, the low-cost commercialization and application of these devices remain great challenges.

To solve the key issues facing light devices, researchers are conducting multimodal studies with various materials, nanostructures, and optical controls. Among the various efforts, nanofiber (NF) technology using unique structures is noteworthy. The NF industry is expected to increase greatly in various areas.[8] In recent years, NFs have been developed and widely applied in many industries, including the electrical, biomedical, physical, and mechanical fields. These applications include light-emitting devices,[9] battery separators,[10] energy storage,[11] functional filters,[12] biodetection systems,[13] membranes,[14] tissue engineering,[15] new types of electrodes,[16] and

DOI: 10.1021/am5075387
ACS Appl. Mater. Interfaces 2015, 7, 68–74

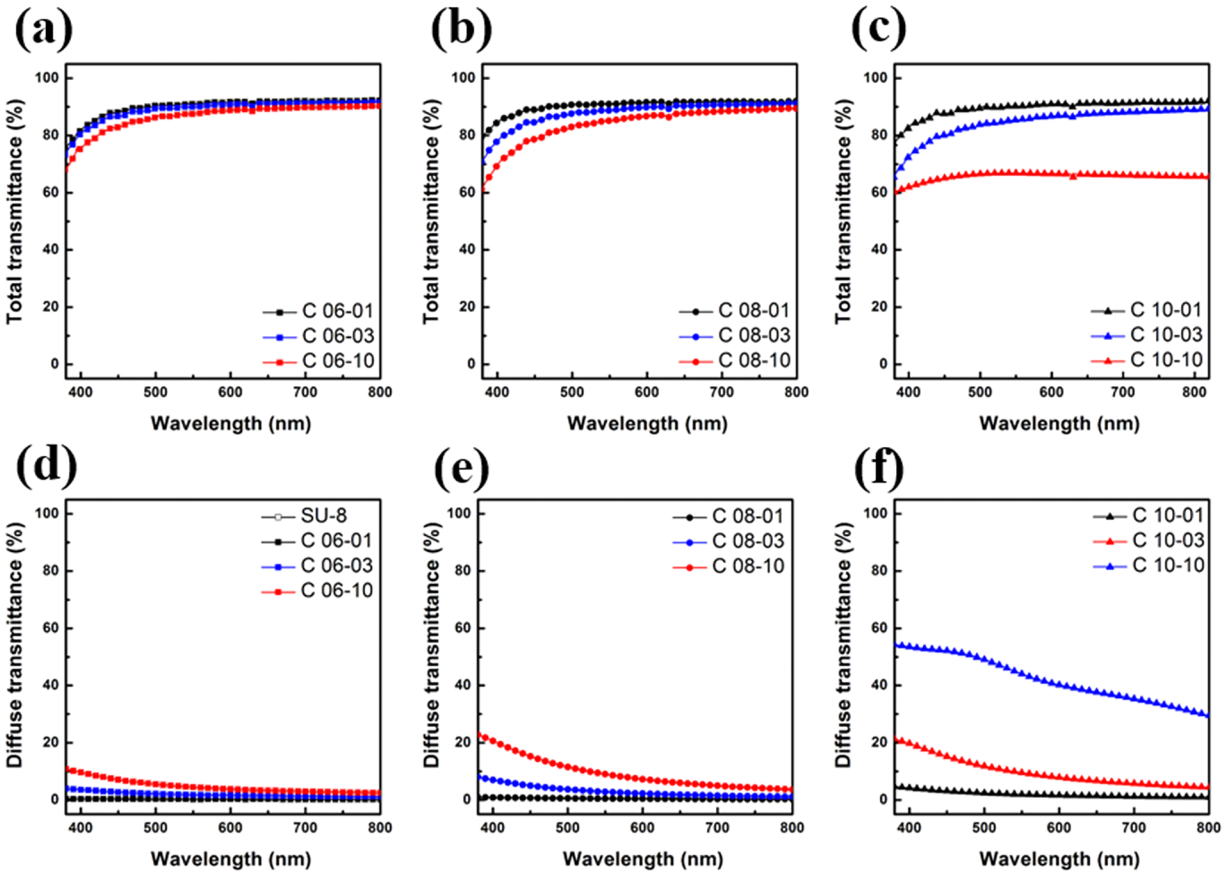

Figure 4. Optical characteristics of PAN NF/SU-8 composite films: (a–c) total optical transmittance, and (d–f) diffuse optical transmittance of various types of composite films.

Table 2. Optical Properties of Various Types of PAN NF/SU-8 Composite Films

sample	total transmittance (%)	parallel transmittance (%)	diffuse transmittance (%)	haze (%)
C 06–01	90.94	90.65	0.29	0.32
C 06–03	90.02	88.24	1.78	1.98
C 06–10	87.58	83.13	4.45	5.08
C 08–01	90.96	90.5	0.46	0.51
C 08–03	88.77	85.96	2.81	3.17
C 08–10	85.14	76.15	8.99	10.56
C 10–01	**90.22**	**88.27**	**1.95**	**2.16**
C 10–03	85.38	75.86	9.52	11.15
C 10–10	**66.85**	**22.77**	**44.08**	**65.93**

alternative flexible substrates.[17] NFs can exhibit various optical, mechanical, and chemical properties, as well as an immense surface area, by the appropriate chemical synthesis. These structural characteristics of NFs can be applied in a wide range of higher value-added businesses.[18]

Such nonwoven polymer NFs were manufactured using various fabrication techniques, depending on their purpose. For example, solution blow spinning,[19,20] melt blowing,[21] centrifugal spinning,[22,23] and wet spinning[24] are generally employed in the industry and laboratories to make nano and submicron nanofibers. Such techniques are valuable for mass production and various applications. Among the various method, electrically assisted spinning (electrospinning) with simple parameter changes (i.e., flow rate and concentration) is a one of the appropriate technique for effective size control of uniform NFs. Also, the electrospinning method can produce high-quality fibers from a liquid and does not require an additional chemical treatment or high-temperature annealing.[25]

Despite their advantages, pristine NFs are inappropriate for optical-electrical and photovoltaic devices owing to a number of fundamental problems, e.g., their surface roughness, weak mechanical adhesion force, low transmittance, and difficulty of handling. To solve the critical problems of pristine NFs, the NF/polymer composite has been introduced.[26] Recent studies of lighting devices[27] fully explain the composite layer, its possible application paradigm, and its potential in future lighting technology. Among the various candidate additional polymers, SU-8 is developed by a photolithography process as a photoresist,[28] to produce high-resolution patterning for micro and nano devices. Thus, the coating condition can be easily controlled. Moreover, the SU-8 exhibits a high optical transparency in the visible radiation area. For this reason, it is employed in different shapes and sizes as a light-outcoupling layer in OLEDs. For example, Bocksrocker et al. fabricated a microspherically textured layer with SiO_2- microspheres/SU-8 attached to an enhanced outcoupling of waveguide and to improve the efficiency of the OLEDs.[29] As mentioned previously, many groups have reported a composite film based on an NF/polymer, and the estimated transparency and mechanical properties pertain to academic achievements rather than actual application.

In this work, we report a newly designed nanosize controlled PAN NF-based composite layer for effective light control with a unique nanostructure, fabricated without any high-temperature

DOI: 10.1021/am5075387
ACS Appl. Mater. Interfaces 2015, 7, 68–74

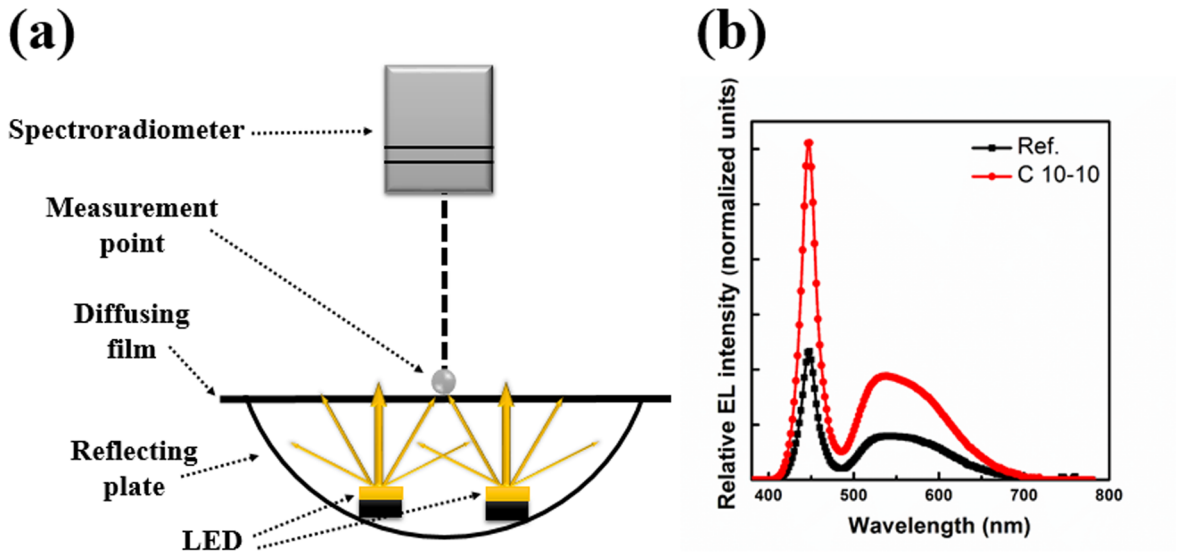

Figure 5. (a) Schematic of the modular laboratory lighting measurement tools to evaluate light diffusion, (b) one-dimensional intensity changes depending on various PAN NF/SU-8 light diffusion films at the accurate midpoint between two LEDs.

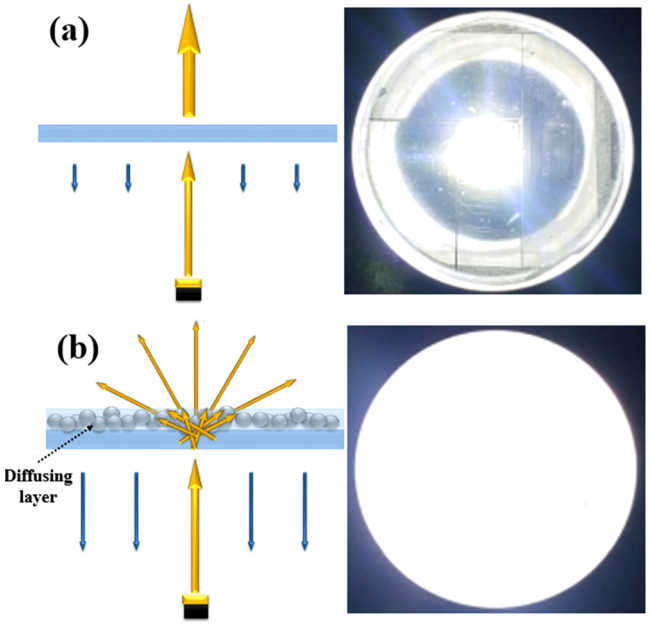

Figure 6. Schematic of antiglare effects mechanisms and photo images of LED light (a) with bare glass and (b) with light diffusion film (C 10−10).

process using plastic or glass deformation. The novel composite layer can be used for various purposes depending on the diameter and cross-linking time of the NFs. The reinforced PAN NF not only exhibited extremely diverse changes in the optical properties because of the diameter difference, but was also applied to LEDs and OLEDs to obtain the ideal EL characteristics.

A schematic of the composite film for the PAN/SU-8 composite film with electrospinning fabrication process is presented in Figure 1. The electrospinning system comprises the high-voltage DC power supply, a spinneret, the syringe pump, and a collector (a grounded conductor).[30] The prepared PAN solution was contained in the syringe, and we used the syringe pump to generate a constant and controllable PAN-solution feed rate. Then, we set up the ring-type collector, and the collected NFs were easily transferred to the substrate. To produce NFs of a fixed size, the flow rates and applied voltages in various PAN solutions were controlled. Subsequently, the SU-8 (SU-8 2002, Micro-Chem) was coated on the transferred NFs. Prepared composite layers were applied in LEDs and OLEDs for their ideal lighting purpose.

We controlled many parameters in order to obtain the appropriate diameter of the NFs, as follows. The PAN solution feed rate was varied from 50 to 200 mL/h, the PAN solution concentration was varied from 6% to 10%, and the applied voltage was varied from 4.5 to 5 kV. The only fixed parameter was the distance between the needle and ring-type collector, which was 10 cm. The diameters of the produced electrospun PAN NF under different manufacturing conditions are summarized in Table 1, and the SEM images of PAN NF are presented in Figure 2 (with different PAN weight ratios of (a, d) 6, (b, e) 8, and (c, f) 10 wt %.) The electrospun NFs were created by a simple production process, without any dangerous chemicals or high-temperature treatments, in contrast with glass and plastic. We evaluated various samples according to the PAN rate percentage (6, 8, 10 wt %) and collecting time (1, 3, 10 min), as shown in Figure 3a−c. In the ordinary case of a pristine PAN NF, as the cross-linking progresses, the heaped NF forms white mats with a low light transmittance, as shown in third line samples of Figure 3d (the pristine PAN NF samples were named in the order "PAN," "rate percentage," and "NF collecting minutes,", respectively). The optical properties of the PAN NF and the declining tendency of the transmittance were caused by the collected milky color NF bunch. Also, the surface conditions of the films cause a significant amount of light scattering, which leads to a deterioration in the total transmittance. NF films that were too thick or heavily stacked exhibited an extremely low transmissivity and were no longer suitable for light systems. Pristine NFs are very vulnerable to external physical influence; the outermost layers are easily damaged, and the whole NF film is peeled back as shown in Figure 3e. Therefore, to control the optical characteristics and achieve a high durability, it is necessary to consider composite-type films.

Among the various candidates, SU-8 is an optically transparent material with a light transmittance of 90% in the wavelength range of 380−780 nm. Therefore, it is widely used in the SU-8 waveguide scattering layer to control light, as shown in Figure 3

DOI: 10.1021/am5075387
ACS Appl. Mater. Interfaces 2015, 7, 68−74

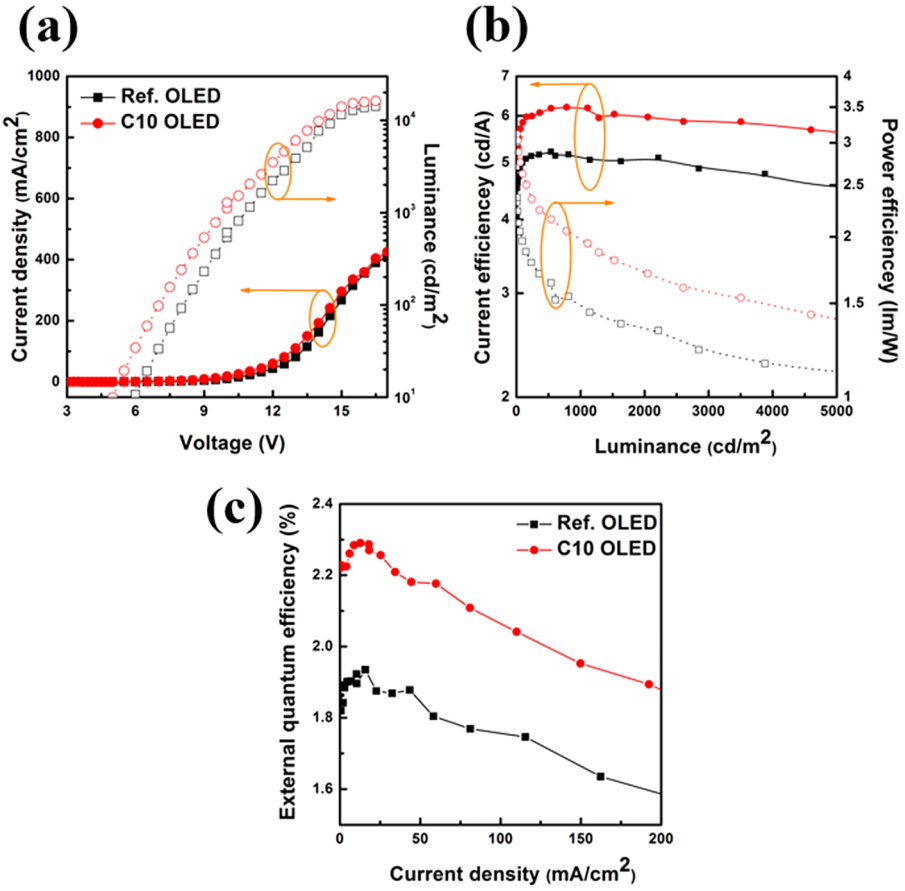

Figure 7. EL characteristics of the OLEDs; (a) current density and luminance as a function of voltage; (b) current efficiency and power efficiency as a function of luminance; (c) external quantum efficiency (EQE) as a function of current density, for reference and C10 OLED.

Table 3. EL Characteristics of the Reference and C10 OLED

			CIE 1931 at 3000 cd/m^2	
device	EQE (%) at 100 mA/cm^2	PE (Im/W) at 3000 cd/m^2	X	Y
ref. OLED	1.76	1.22	0.31	0.53
C 10 OLED	2.06	1.57	0.31	0.52
	(+17%)	**(+29%)**	**(Δ 0.00)**	**(Δ 0.01)**

(composite PAN NF/SU-8 samples were named in the order "C," "rate percentage," and "NF collecting minutes,", respectively). We fabricated the composite PAN NF/SU-8 to increase the strength and compensate for the weakness of the pristine NFs. Notably, after the white PAN NFs were buried in the SU-8 layer, the PAN NF/SU-8 composites film exhibited a drastically increased total light transmittance. The highest increases were observed in the PAN 08−10 sample, which exhibited a total visible light transmittance of up to 80%. After the SU-8 was coated on the NF samples, the almost-composite samples exhibited a similar trend, improving to over 75% in transparency. For this increase, the SU-8 entirely covered the transferred NF layer, thereby filling the empty areas between the NFs and thus strongly binding the PAN NF and reducing the total light transmittance without a high-temperature treatment. Indeed, almost various composite film samples exhibited an excellent light transmittance of over 80% (Figure 4a−c), which is nearly the transmittance of the SU-8 film, indicating that the embedded NFs have little effect on the loss of the total transmitted light with under 10% diffuse transmittance (Figure 4d−f). Viewed from the other side, these small effects have an enormous impact inside the composite layer. Optical properties of all samples (totally transmitted, parallel light, amount of diffuse light, and haze) are summarized in Table 2.

However, close inspection reveals that the C 10−10 sample (SU-8 covering PAN 10−10) exhibited an exceptional loss in the total transmittance, which is wavelength-dependent. This is unlikely to be reversible, despite the composition with SU-8. Although the C 10−10 sample exhibited a noticeably low total transmittance of 67% and high diffuse transmittance of 44%, owing to the high haze value of 66% and the parallel transmittance of under 23% (in 550 nm wavelength), the milky-glass optical property could be used to make the illumination LED light diffusion suitable without a glare effect from the direct light transmission. The optical properties of various composite films were measured using modular laboratory lighting measurement tools. Two LEDs were placed next to each other and 2 cm behind the light diffusion film, and a spectroradiometer was placed in front of the light system to measure the light diffused by the various films, as shown in Figure 5a. Comparing the light diffusion effect among various light diffusion samples indicates the relative intensity according to the light diffuse films; the C10−10 sample exhibits the highest EL intensity, as shown in Figure 5b. In contrast, the LED light with the reference sample (bare glass) showed no significant light diffusion effect. In general, the brightness of the LED light source at the center was comparatively greater than that at the side as was expected. Thus, obviously the high-haze light diffusion film plays a central role in achieving uniform light distribution from

DOI: 10.1021/am5075387
ACS Appl. Mater. Interfaces 2015, 7, 68−74

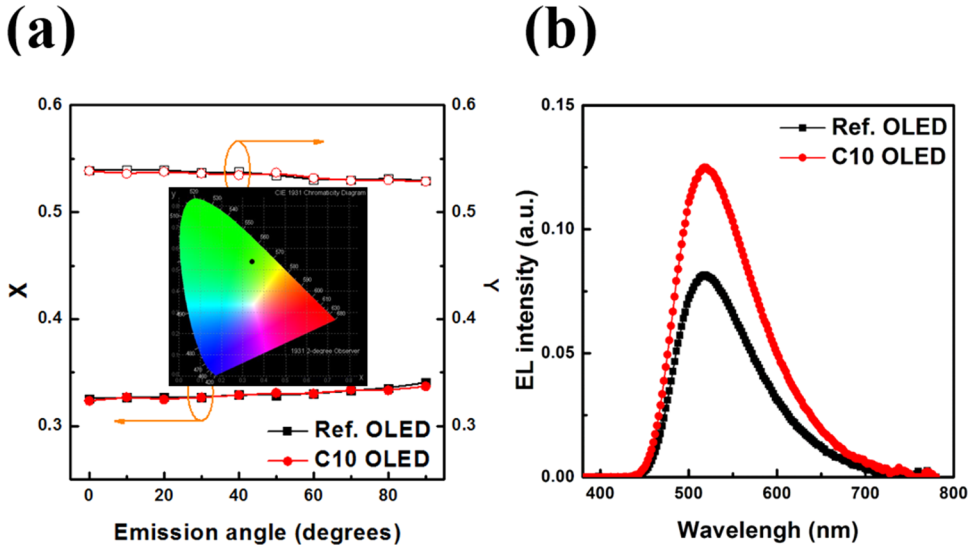

Figure 8. (a) CIE color coordinate emission as a function of the angle for reference and C10 OLED and CIE 1931 color coordinates of C10 OLED, (b) emission spectra measured from surface normal at a current density of 100 mA/cm^2 for reference and C10 OLED.

the center to the side position for controlling the uniformity of the illumination in the LED light system. This measurement of the intensity at the accurate midpoint between the two LED lights clearly indicates the light distribution of the effective diffusion films due to the diffused light rather than the direct parallel light intensity. Figure 6a, b show schematic of antiglare effects mechanisms and photos of LED lights with the bare glass and light diffusion film (C 10−10). These results definitely indicate light diffuser layer properties, according to the required optical characteristics that can be easily designed with the appropriate components for the lighting system. Moreover, we not only avoided the glare effect but also proved the possibility of a relatively equal light distribution.

On the other hand, NF-embedded unique-structure films with a high transmittance were introduced for the light-outcoupling efficiency enhancement of the OLEDs. Unlike the other films of a high transmittance, the C 10−01 film had a light diffusion transmittance of 2% while maintaining a high total light transmission.

To create more high scattering effect for efficiency enhancement of OLEDs, we applied C 10−01 films to the OLEDs (C10 OLED) and evaluated. Figure 7 indicates the EL characteristics of the fabricated C10 OLED and a reference, and their device performances are summarized in Table 3. Figure 7a indicates the current density and luminance as functions of the applied voltage. The current density of the C10 OLED is nearly identical to that of the reference OLED at the same bias voltage because the C10 OLED has the same structure composition as the reference OLED, except for the C 10−10. However, as shown in Figure 7b, the power efficiencies of the fabricated C10 and reference OLED were 1.57 and 1.22 lm/W, respectively, and their current efficiencies were 5.86 and 4.88 cd/A, respectively, at a luminance of 3000 cd/m^2. The external quantum efficiency (EQE) of the C10 OLED was 2.06% at a current density of 100 mA/cm^2, as shown in Figure 7c. These results indicate an increase in the power efficiency and EQE of C10 OLED, as functions of the current density, caused by the C 10−01 film, compared with the reference OLED. For multilateral analysis, the changes in the International Commission on Illumination (CIE) color coordinates and the emission angle in the reference and C10 OLED. When the emission angle was increased from 0 to 90 deg, the CIE color coordinates of the C10 OLED shifted from (0.324, 0.539) to (0.337, 0.529). The variations in the x and y color coordinates were 0.003 (0.92%) and 0.01 (1.86%); these color coordinates exhibit a trend similar to the reference OLED, as shown in Figure 8a. Thus, it is definitively proved that the C10−01 film does not affect the light distortion in all angles. The EL spectra of the reference and C10 OLED at a current density of 100 mA/cm^2 are presented in Figure 8b. The EL spectra enhancement in the C10 OLED appears over the entire EL spectrum. The reference and C10 OLED exhibit similar EL spectra at the same front viewing angle, which clearly indicates the enhanced light emission by the C 10−10 of the NF-embedded unique composite layer without a shift in the EL spectrum of the device. The present results confirm a simple, low-cost, and low-temperature technique for improving the EL efficiency of OLEDs.

In conclusion, we demonstrated a novel PAN NF-based composite layer to realize the ideal optical properties of various lighting devices, using asymmetric nanostructures for high light scattering and prevent distortion of the light. Our newly designed novel composite layer will take advantage of various lighting systems, depending on the composition rate and thickness, with the appropriate optical efficiency. In particular, differences in the NF diameter cause different optical characteristics, representing the light transmittance characteristics with a certain trend. We observed various optical properties, including low parallel light transmittance values and higher haze values without the glare effect from direct light sources. This was applied to the white light LED for an effective illumination light diffusion layer. Also, in the case of OLEDs, PAN NF/SU-8 films were fabricated as a light-scattering layer to improve the EL characteristics and exhibited light extraction enhancement properties.

These results indicate that the uniquely designed novel PAN NF/SU-8 composite film provides effective modulation of light properties and sufficient illumination quality for various lighting applications and that it has great potential for utilization as well as commercial success in mass production.

DOI: 10.1021/am5075387
ACS Appl. Mater. Interfaces 2015, 7, 68−74

■ ASSOCIATED CONTENT

Supporting Information

Details of experiments, characterization, and device fabrication described in the text. This material is available free of charge via the Internet at http://pubs.acs.org

■ AUTHOR INFORMATION

Corresponding Authors

*E-mail: zerook@korea.ac.kr.
*E-mail: bkju@korea.ac.kr.

Author Contributions

Y.W.P. and B.-K.J. contributed equally to this work.

Notes

The authors declare no competing financial interest.

■ ACKNOWLEDGMENTS

This research was supported by the Basic Science Research Program through the National Research Foundation of Korea (NRF), funded by the Ministry of Education, Science and Technology (2012R1A6A3A04039396), an NRF grant funded by the Korean government (MSIP) (CAFDC 4−2, NRF 2007−0056090), and the Industy technology R&D program of MOTIE/KEIT. [10048317, Development of red and blue OLEDs with external quantum efficiency over 20% using delayed fluorescent materials]. The authors thank the staff of KBSI for technical assistance.

■ REFERENCES

(1) Salamon, A. W. The Current World of Nanomaterial Characterization: Discussion of Analytical Instruments for Nanomaterial Characterization. *Environ. Eng. Sci.* **2013**, *30*, 101−108.

(2) Chang, M. H.; Das, D.; Varde, P. V.; Pecht, M. Light Emitting Diodes Reliability Review. *Microelectron. Reliab.* **2012**, *52*, 762−782.

(3) Geffroy, B.; le Roy, P.; Prat, C. Organic Light-emitting Diode (OLED) Technology: Materials, Devices and Display Technologies. *Polym. Int.* **2006**, *55*, 572−582.

(4) Behar-Cohen, F.; Martinsons, C.; Viénot, F.; Zissis, G.; Barlier-Salsi, A.; Cesarini, J. P.; Enouf, O.; Garcia, M.; Picaud, S.; Attia, D. Light-emitting Diodes (LED) for Domestic Lighting: Any Risks for the Eye? *Prog. Retinal Eye Res.* **2011**, *30*, 239−257.

(5) Hyun, W. J.; Im, S. H.; Park, O. O.; Chin, B. D. Corrugated Structure Through a Spin-Coating Process for Enhanced Light Extraction from Organic Light-Emitting Diodes. *Org. Electron.* **2012**, *13*, 579−585.

(6) Lee, C.; Kim, J. J. Enhanced Light Out-coupling of OLEDs with Low Haze by Inserting Randomly Dispersed Nanopillar Arrays Formed by Lateral Phase Separation of Polymer Blends. *Small* **2013**, *9*, 3858−3863.

(7) Kim, J. W.; Jang, J. H.; Oh, M. C.; Shin, J. W.; Cho, D. H.; Moon, J. H.; Lee, J. I. FDTD Analysis of the Light Extraction Efficiency of OLEDs with a Random Scattering Layer. *Opt. Express.* **2014**, *22*, 498−507.

(8) Cho, H.; Min, S. Y.; Lee, T. W. Electrospun Organic Nanofiber Electronics and Photonics. *Macromol. Mater. Eng.* **2013**, *298*, 475−486.

(9) Ummartyotin, S.; Juntaro, J.; Sain, M.; Manuspiya, H. Development of Transparent Bacterial Cellulose Nanocomposite Film as Substrate for Flexible Organic Light Emitting Diode (OLED) Display. *Ind. Crops Prod.* **2012**, *35*, 92−97.

(10) Cho, T. H.; Sakai, T.; Tanase, S.; Kimura, K.; Kondo, Y.; Tarao, T.; Tanaka, M. Electrochemical Performances of Polyacrylonitrile Nanofiber-based Nonwoven Separator for Lithium-ion Battery. *Electrochem. Solid-State Lett.* **2007**, *10*, A159−A162.

(11) Mao, X.; Alan Hatton, T.; Rutledge, G. C. A Review of Electrospun Carbon Fibers as Electrode Materials for Energy Storage. *Curr. Org. Chem.* **2013**, *17*, 1390−1401.

(12) Hung, C. H.; Leung, W. W. F. Filtration of Nano-aerosol Using Nanofiber Filter under Low Peclet Number and Transitional Flow Regime. *Sep. Purif. Technol.* **2011**, *79*, 34−42.

(13) Periyakaruppan, A.; Arumugam, P. U.; Meyyappan, M.; Koehne, J. E. Detection of Ricin Using a Carbon Nanofiber Based Biosensor. *Biosens. Bioelectron.* **2011**, *28*, 428−433.

(14) Huang, F. L.; Wang, Q. Q.; Wei, Q. F.; Gao, W. D.; Shou, H. Y.; Jiang, S. D. Dynamic Wettability and Contact Angles of Poly(vinylidene fluoride) Nanofiber Membranes Grafted with Acrylic Acid. *eXPRESS Polym. Lett.* **2010**, *4*, 551−558.

(15) Wang, F.; Liu, X. Recent Advances in the Chemistry of Lanthanide-doped Upconversion Nanocrystals. *Chem. Soc. Rev.* **2009**, *38*, 976−989.

(16) Guo, H.; Lin, N.; Chen, Y.; Wang, Z.; Xie, Q.; Zheng, T.; Gao, N.; Li, S.; Kang, J.; Cai, D.; Peng, D. L. Copper Nanowires as Fully Transparent Conductive Electrodes. *Sci. Rep.* **2013**, 3.

(17) Yan, X.; Tai, Z.; Chen, J.; Xue, Q. Fabrication of Carbon Nanofiber-polyaniline Composite Flexible Paper for Supercapacitor. *Nanoscale* **2011**, *3*, 212−216.

(18) Long, Y. Z.; Yu, M.; Sun, B.; Gu, C. Z.; Fan, Z. Recent Advances in Large-scale Assembly of Semiconducting Inorganic Nanowires and Nanofibers for Electronics, Sensors and Photovoltaics. *Chem. Soc. Rev.* **2012**, *41*, 4560−4580.

(19) Zhuang, X.; Yang, X.; Shi, L.; Cheng, B.; Guan, K.; Kang, W. Solution Blowing of Submicron-scale Cellulose Fibers. *Carbohydr. Polym.* **2012**, *90*, 982−987.

(20) Behrens, A. M.; Casey, B. J.; Sikorski, M. J.; Wu, K. L.; Tutak, W.; Sandler, A. D.; Kofinas, P. In Situ Deposition of PLGA Nanofibers via Solution Blow Spinning. *ACS Macro Lett.* **2014**, *3*, 249−254.

(21) Yarin, A. L.; Sinha-Ray, S.; Pourdeyhimi, B. Meltblowing: Multiple Polymer Jets and Fiber-size Distribution and Lay-down Patterns. *Polymer.* **2011**, *52*, 2929−2938.

(22) Vazquez, B.; Vasquez, H.; Lozano, K. Preparation and Characterization of Polyvinylidene Fluoride Nanofibrous Membranes by Forcespinning. *Polym. Eng. Sci.* **2012**, *52*, 2260−2265.

(23) Rane, Y.; Altecor, A.; Bell, N. S.; Lozano, K. Preparation of Superhydrophobic Teflon® AF 1600 Sub-micron Fibers and Yarns Using the Forcespinning Technique. *J. Eng. Fibers Fabr.* **2013**, *8* (4), 88−95.

(24) Ma, R.; Lee, J.; Choi, D.; Moon, H.; Baik, S. Knitted Fabrics Made From Highly Conductive Stretchable Fibers. *Nano Lett.* **2014**, *14*, 1944−1951.

(25) Wu, H.; Hu, L.; Rowell, M. W.; Kong, D.; Cha, J. J.; McDonough, J. R.; Zhu, J.; Yang, Y.; McGehee, M. D.; Cui, Y. Electrospun Metal Nanofiber Webs as High-performance Transparent Electrode. *Nano Lett.* **2010**, *10*, 4242−4248.

(26) Pandey, J. K.; Nakagaito, A. N.; Takagi, H. Fabrication and Applications of Cellulose Nanoparticle-based Polymer Composites. *Polym. Eng. Sci.* **2013**, *53*, 1−8.

(27) Kim, J.; Noh, J.; Jo, S.; Park, K. E.; Park, W. H.; Lee, T. S. Simple Technique for Spatially Separated Nanofibers/Nanobeads by Multi-nozzle Electrospinning Toward White-light Emission. *ACS Appl. Mater. Interfaces* **2013**, *5*, 6038−6044.

(28) Del Campo, A.; Greiner, C. SU-8: A Photoresist for High-aspect-ratio and 3D Submicron Lithography. *J. Micromech. Microeng.* **2007**, *17*, R81−R95.

(29) Bocksrocker, T.; Hoffmann, J.; Eschenbaum, C.; Pargner, A.; Preinfalk, J.; Maier-Flaig, F.; Lemmer, U. Micro-spherically Textured Organic Light Emitting Diodes: A Simple Way Towards Highly Increased Light Extraction. *Org. Electron.* **2013**, *14*, 396−401.

(30) Li, D.; Xia, Y. Electrospinning of Nanofibers: Reinventing the Wheel? *Adv. Mater.* **2004**, *16*, 1151−1170.

DOI: 10.1021/am5075387
ACS Appl. Mater. Interfaces 2015, 7, 68−74